2019

Stochastic vs. Deterministic Scheduling of a Combined Natural Gas and Power System with Uncertain Wind Energy

Dan Hu, *Iowa State University*
Sarah M. Ryan

Stochastic vs. Deterministic Scheduling of a Combined Natural Gas and Power System with Uncertain Wind Energy

Dan Hu, Sarah M. Ryan, *

September 18, 2018

Abstract

We compare approaches for addressing uncertainty in the joint scheduling of a combined power and gas system, with the goal of minimizing the total cost of meeting demands for gas and electricity, while satisfying operational and equilibrium constraints. A stochastic programming model and a deterministic model with reserves are formulated to investigate the hourly unit commitment and economic dispatch in the power system as well as the hourly working schedule of the natural gas system. The deterministic model uses reserves proportional to the wind energy forecast to mitigate the effect of the uncertainty in wind energy, whereas the stochastic programming model makes the day-ahead decisions while explicitly considering the wind energy uncertainty. Nonlinear constraints on the gas flows in pipelines are linearized with binary variables where, based on numerical experimentation, the number of piecewise linear segments is chosen to balance accuracy and computational efficiency. A six-bus power system with seven-node gas system and the IEEE 24-bus power system with adjusted Belgian 20-node gas system are analyzed. The simulation results indicate that, when the total wind capacity exceeds 15% of the conventional generation capacity, the stochastic programming model produces schedules with comparable or lower cost and energy shortages than the deterministic model with reserves.

Keywords: Natural gas system, Power system, Short-term unit commitment and economic dispatch, Wind energy.

1 Introduction

According to a U.S. government forecast, the share of natural gas in the total electricity generation will rise from 27% in 2012 to 31% in 2040, while the share from coal will decrease from 39% to 34% [1]. This

*D. Hu and S. Ryan are with the Department of Industrial and Manufacturing Systems Engineering, Iowa State University, Ames, IA 50011-2164 USA. (Email: danhu@iastate.edu, smryan@iastate.edu)

change results from the retirement of coal-fired generators, the development of high-efficiency natural gas fueled power generators (NGPGs), the increase of natural gas supply with a relatively stable gas price since 2009, and potential emission regulations. To maintain a reliable power system, more research about how to make unit commitment (UC) and economic dispatch (ED) decisions for the increasing numbers of NGPGs is needed.

Wind energy, with a low operational cost, can be added into the power grid directly and thus relieve some of the pressure on NGPGs. Meanwhile, NGPGs can ramp their production up and down quickly according to the variable wind energy. The cooperation of the wind generators and NGPGs can not only decrease the operational cost but also increase the reliability of the grid. Due to the pre-schedule scheme of natural gas and power systems, ahead of the actual operating day, decisions about the supply of natural gas must be made on the basis of wind power output forecasts. If the actual wind output is less than the forecast, load shedding may occur if too few units are committed or not enough gas is available. Thus, it is important to plan the operation of the natural gas and power systems accounting for the uncertainty of wind energy.

Currently in many parts of the world, the natural gas and power systems are operated independently. As natural gas claims a higher share of generation capacity, more generating companies consider signing firm contracts with the natural gas suppliers to make sure they have sufficient fuel. Because the peak gas and electricity loads may overlap and coincide with extreme weather, the current independent operation of the natural gas and power systems makes it hard to react to these conditions. Recently, the U.S. Federal Energy Regulatory Commission, which regulates both systems, mandated adjustments in the timing of day-ahead wholesale electricity markets to permit better coordination with the gas market. Here, we examine the combined operation of the electric power and natural gas systems to minimize the total operational cost including penalties on non-served energy.

In this paper, we focus on comparing the stochastic and the deterministic scheduling of the combined natural gas and power system with uncertain wind energy. We formulate the problem with a centralized direct current (DC) power flow model and static natural gas system, neglecting some complicated dynamic power and natural gas constraints for the sake of tractability. Uncertainty in the wind energy is incorporated by adding fixed reserves in the deterministic model or by probabilistic scenarios in the stochastic programming (SP) model. Here we quantify *risk* as the expected unserved energy (in the form of either gas or electricity) and *cost* as the UC and expected production cost in the combined system. While some previous comparisons of stochastic and deterministic scheduling of these systems together have focused on expected cost, we examine risk impacts more closely. We compare the cost and risk in numerical case studies, illustrating that under deep penetration of wind power, the SP model reduces both cost and risk compared to the deterministic model with reserves.

2 Literature Review

Many researchers have discussed approaches to modeling the combined natural gas and power system. The effects of gas infrastructure and gas unit price on power generation scheduling were addressed by using security-constrained unit commitment (SCUC) [2]. Dual decomposition, Lagrangian relaxation and dynamic programming were used to solve a large scale integrated electricity-gas optimal short-term planning problem with a hydrothermal system included, formulated as a nonlinear mixed-integer program [3], while a day-ahead integrated SCUC model is applied incorporating the natural gas network constraints and fuel diversity as an effective peak shaving strategy [4]. Reference [5] applied Benders decomposition in the SCUC problem with natural gas transmission constraints and reference [6] formulated a bi-level model in which the upper level problem includes the unit commitment (UC) and economic dispatch (ED) problems while the lower level problem concerns the natural gas system. With a focus on component outages, or contingencies, a coordinated stochastic model, including scenarios of random generating unit and line outages, was proposed to demonstrate that hourly economic demand response would decrease the dependence on natural gas constraints for the optimal operation of the electric power system [7]; a two-stage stochastic programming model of the UC with natural gas constraints, in which the first stage optimizes the UC and gas production decisions, was developed [8]; and reference [9] applied the corresponding linear sensitivity analysis to adjust decisions in advance for system security in the event of a single contingency. The Alternating Direction Method of Multipliers (ADMM) was used not only to solve the gas-electric integrated optimal power flow model and compare the results with and without a coordinating operator [10] but also to coordinate the gas-electric systems and demonstrate the algorithm efficiency, under electric load uncertainty [11]. In [12], second-order cone constraints are employed as a relaxation for the non-convex gas flow through pipelines and a sensitivity analysis of the wind energy forecast error is conducted. Reference [13] applied the energy modeling method to the different energy systems including the natural gas system, power system, gas-to-power units, gas-to-power units and line pack of the natural gas. Reference [14] proposed a genetic algorithm based hybrid model for a power system distribution network, a natural gas network and the energy centers including the combined heat and power units, different energy conversion devices and demand responsive load to minimize the day-ahead operational cost of the integrated urban energy system, but the optimality is not guaranteed. Moreover, it is difficult to extend these methodologies to multiple scenarios due to their low computational efficiency. A study of a distribution system including reverse power management focuses on the operation of the power-to-gas and gas-to-power facilities [15]. Reference [16] investigated the micro integrated electric power, natural gas and heat delivery system and focused on minimizing the total operation and environmental cost, and reference [17] proposed a robust optimization model of the integrated natural

gas and power system model with uncertain wind energy and focused on the worst cases. None of references [15], [16] and [17] modeled the detailed non-convex gas flow through pipelines.

Several papers presented models of gas flows in pipelines. For the most general case of transient flow, the laws of conservation of mass, energy and momentum were applied to find three partial differential equations (PDEs) [18]. However, although the gas state condition could be added to those three PDEs to help identify a closed form of the solution, more equations are required due to the large number of variables in the transient model. The theoretical and some experimental results of the unsteady and transient flow of compressible fluids in pipelines were reviewed in [19]. Given the special physical characteristics of gas pipelines, they proposed a unidirectional flow model and developed various derivative models of different thermal conditions. A one-dimensional, non-isothermal gas flow model was solved to simulate the slow and fast fluid transients and address the effect of various thermal models on the flow rate, pressure and temperature in the pipelines [20]. Given a one dimensional homo-thermal steady state flow condition, the PDEs for transient state flow could be simplified and the Weymouth equation (WE) was proposed to model gas flow in passive pipelines [6]. A theoretical and computational comparison of piecewise linear models for approximating the WEs led to the conclusion that the incremental method, where continuous variables are introduced to represent the portion of each segment and binary variables force all intervals to its left must be completely used if a segment is chosen, is the fastest [21]. The non-convex Weymouth gas flow equation was relaxed to convexified quadratic constraints to enable solution of the optimal gas flow by an iterative second-order cone programming procedure with a greater efficiency than traditional nonlinear methods [22]. A robust co-optimization scheduling model was proposed to study the coordinated natural gas and power system while considering key power system uncertainties [23], which only mentions incremental method is used for linearizing nonlinear constraints but the computational efficiency and accuracy for different numbers of segments were not discussed.

UC and ED formulations traditionally have been based on fixed reserve limits. With the power turbine technology development, the capacity of wind turbines has increased significantly and wind power has become an important energy resource. Thus, methodologies for incorporating increasing amounts of wind energy into the power system attract more attention. Although many research studies have been done on scheduling the combined natural gas and power system as well as on the UC/ED problems with uncertain wind energy, there are few studies on the combined natural gas and power system that also include uncertain wind energy. Reference [24] formulated a coordinated stochastic day-ahead scheduling model of the electricity infrastructure with costs and constraints imposed by the gas system and examined its ability to firm the uncertain wind energy. This study did not compare the stochastic programming approach against traditional methods of adding reserves and did not analyze different levels of wind uncertainty. Reference [25] describes

the study that, to our knowledge, is most similar to this one. The authors compared deterministic, two-stage, and multi-stage stochastic formulations of commitment and dispatch of an integrated gas and electricity network. However, they separately solved a (stochastic) mixed-integer program to schedule the electricity generators and a nonlinear program to determine if gas demands could be satisfied under that schedule, then iteratively applied a heuristic method to constrain the gas generators' output, re-solving both models until feasibility could be achieved.

We apply linear approximations to the gas constraints and integrate the decisions for both systems in a single optimization model. By penalizing energy- and gas-balance constraint violations in the objective function, we quantify the risk of load shedding in either system. The contributions of this paper are:

(1) We model the combined day-ahead scheduling of the natural gas and power systems with reserves. The current deterministic models for the integrated natural gas and power system in the literature include only the wait-and-see model and the expected value model, which are special cases of the stochastic programming model. There is a theoretically guaranteed relationship among the optimal expected costs of solution to stochastic model, wait-and-see model and the expected value model. However, our proposed deterministic model with reserves is a different and more practical model, where reserves are added in the day ahead market, and there is no guarantee that the stochastic programming model dominates it. Thus, it is important to compare the results of the deterministic model with reserves and the stochastic programming model. In numerical case studies, the stochastic program results in less cost and risk when the wind uncertainty is high.

(2) We compare the performance of a stochastic program and a deterministic optimization with reserve constraints (called a DR model) when confronted with different levels of wind energy uncertainty on different days. Current research only tests one or two cases of uncertainty using sensitivity analysis, which does not guarantee the generality of the conclusions.

(3) We experiment with different numbers of segments when linearizing the nonlinear Weymouth equation, to identify a number of segments that best balances computational efficiency with accuracy. Because the past publications each use a single number of piecewise segments, which varies among them, it is hard to compare their results. The number of segments we identify can serve as a standard for future studies.

The remainder of this paper has the following structure. The two models are presented along with a perfect information (wait and see) model to evaluate their effectiveness in Section 3. Section 4 describes the scenario generation process and numerical simulations to compare the operational cost and risk of the SP and DR models. Finally, the conclusions are summarized in Section 5.

3 Model

Although gas and electricity can flow in either direction through a pipeline or transmission line, respectively, we model those components as directed arcs either from or to a node, where negative values for corresponding flow variables indicate flows in the reverse direction. Define the notation as follows:

Sets and indices

$\mathcal{J}$	Gas nodes, indexed by j
$\mathcal{J}'(j)$	Gas nodes connected to j by passive pipelines from j, indexed by j'
$\mathcal{J}''(j)$	Gas nodes connected to j by passive pipelines to j, indexed by j''
$\mathcal{C}'(j)$	Gas nodes connected by active pipelines from j, indexed by c'
$\mathcal{C}''(j)$	Gas nodes connected by active pipelines to j, indexed by c''
$\Lambda(j)$	Gas wells in node j, indexed by λ; $\Lambda = \bigcup_{j\in\mathcal{J}} \Lambda(j)$ is the set of all gas wells
$\Psi(j)$	Storage facilities in node j, indexed by ψ; $\Psi = \bigcup_{j\in\mathcal{J}} \Psi(j)$ is the set of all storage facilities.
$\mathcal{I}$	Electricity nodes, indexed by i and i'
$\mathcal{I}'(i)$	Electricity nodes connected to i by a transmission line from i, indexed by i'
$\mathcal{I}''(i)$	Electricity nodes connected to i by a transmission line to i, indexed by i''
$\mathcal{G}(i,j)$	Gas-fired generators at power node i and gas node j, indexed by g; $\mathcal{G} = \bigcup_{i\in\mathcal{I},j\in\mathcal{J}} \mathcal{G}(i,j)$ is the set of all gas-fired generators.
$\mathcal{N}(i)$	Non-gas-fired conventional generators at node i, indexed by n; $\mathcal{N} = \bigcup_{i\in\mathcal{I}} \mathcal{N}(i)$ is the set of all non-gas-fired generators.
$\mathcal{W}(i)$	Wind turbines at node i, indexed by w; $\mathcal{W} = \bigcup_{i\in\mathcal{I}} \mathcal{W}(i)$ is the set of all wind turbines
$\mathcal{M}$	Set of all gas-fired and non-gas-fired generators, indexed by m; $\mathcal{M} = \mathcal{G} \cup \mathcal{N}$
$\mathcal{T}$	Hours from 1 to $\lvert\mathcal{T}\rvert$, indexed by t
$\mathcal{S}$	Wind energy scenarios, indexed by s
$\mathcal{K}$	Piecewise segments of gas flow quantities, indexed by k

Binary Decision Variables

$u_{g,t}, u_{n,t}, u_{m,t}$	Unit commitment indicator: equals 1 if unit is online in hour t and 0 otherwise
$y^k_{j,j',t}$	Linearization segment indicator

Nonnegative Continuous Decision Variables

$v^u_{g,t}, v^u_{n,t}, v^u_{m,t}$	Unit start-up indicator: equals 1 if the unit is started up in hour t and 0 otherwise
$v^d_{g,t}, v^d_{n,t}, v^d_{m,t}$	Unit shut-down indicator: equals 1 if the unit is shut down in hour t and 0 otherwise
p^{ng}_{λ}	Daily natural gas production level [kcf/day]
$\pi_{j,t}$	Gas pressure squared [Psig^2]
$\delta^k_{j,j',t}$	Linear approximating coefficients for passive pipelines
$\alpha^-_{j,t,s}$,$\alpha^+_{j,t,s}$	Unserved/excess gas in gas node j [kcf]
$l_{\psi,t,s}$	Storage level [kcf]
$q^{out}_{\psi,t,s}, q^{in}_{\psi,t,s}$	Out/in-flow of storage facility [kcf/h]
$p_{g,t,s}, p_{n,t,s}, p_{m,t,s}$	Electricity production [MWh]
$\mu_{g,t,s}$	Gas demand for electricity generation [kcf/h]
$p^{wind}_{w,t,s}$	Wind energy output [MWh]
$r_{g,t}, r_{n,t}, r_{m,t}$	Operating reserves [MWh]
$\beta^-_{i,t,s}$,$\beta^+_{i,t,s}$	Unserved/excess electricity [MWh]
$\gamma^-_{t,s}$,$\gamma^+_{t,s}$	Non-supplied/excess reserves [MWh]

Unrestricted Continuous Decision Variables

$\eta_{j,j',t}$	Gas flow from j to j' [kcf]
$\Delta\pi_{j,j',t}$	Gas squared pressure difference between j and j' [Psig^2]
$\theta_{i,t,s}$	Phase angle [rad]
$f_{i,i',t,s}$	Line flow from i to i' [MWh]

Fixed Parameters

$D_{j,t}^{ng}$	Non-electric gas demand [kcf/h]
$\overline{P}_{\lambda}^{ng}, \underline{P}_{\lambda}^{ng}$	Max/Min daily gas production [kcf/day]
$C_{\lambda}^{ng}, C_{\psi}^{stor}$	Gas production/storage cost [$/kcf]
$C_{j,j'}$	Passive pipeline constant [kcf/Psig]
$\tau_{j,c'}$	Max squared pressure increase ratio of active pipelines
$\overline{\pi}_j, \underline{\pi}_j$	Max/Min squared pressure [Psig^2]
$\Delta\pi_{j,j'}^{k}$	Squared pressure gap of the segment
$\overline{L}_{\psi}, \underline{L}_{\psi}$	Max/Min storage level [kcf]
Q_{ψ}	Max net flow (outflow minus inflow) [kcf]
$\eta_{j,j'}^{k}$	Gas flow of the k^{th} piecewise segment on pipeline from j to j'
$\Gamma_{\alpha}^{-}, \Gamma_{\alpha}^{+}$	Unserved/excess gas penalty [$/kcf]
ϕ_g	Efficiency of gas generator [kcf/MWh]
$C_g^{sd}, C_g^{su}, C_n^{sd}, C_n^{su}, C_m^{sd}, C_m^{su}$	Shut-down/start-up cost [$]
C_n^{prod}	Power production cost [$/MWh]
$\Gamma_{\beta}^{-}, \Gamma_{\beta}^{+}$	Unserved/excess electricity penalty [$/MWh]
$\Gamma_{\gamma}^{-}, \Gamma_{\gamma}^{+}$	Non-supplied/excess reserves penalty [$/MWh]
$\overline{P}_g, \underline{P}_g, \overline{P}_n, \underline{P}_n, \overline{P}_m, \underline{P}_m$	Max/min electricity generation [MWh]
$R_g^{up}, R_n^{up}, R_m^{up}, R_g^{down}, R_n^{down}, R_m^{down}$	Max ramp up/down rate [MW]
$X_{i,i'}$	Transmission line impedance [pu]
$T_g^{on}, T_n^{on}, T_m^{on}, T_g^{off}, T_n^{off}, T_m^{off}$	Min on/off time [h]
$D_{i,t}^{e}$	Electricity demand forecast [MWh]
$\overline{F}_{i,i'}$	Max line flow [MWh]
$\hat{P}_{w,t}^{wind}$	Available wind energy forecast [MWh]
WR	Reserve margin for wind energy [%]

Uncertain Parameters

$\overline{P}_{w,t,s}^{wind}$	Available wind energy in scenario s [MWh]
ξ_s	Scenario probability

3.1 Stochastic Programming (SP) Model

We propose a two-stage stochastic mixed-integer linear programming (SP) model of scheduling the combined energy system to satisfy demands for electricity and gas under uncertain wind energy supply. The two stage model not only deals with the uncertainties in the short-term scheduling problem, but also reflects the difference in time scales for operating inflexible thermal units and adjusting to varying amounts of load and wind energy. As in many two-stage stochastic unit commitment models, we consider decisions on an hourly basis. To avoid the end of day distortions in the decisions, we minimize the expected cost over a 36-hour study horizon to be implemented over a 24-hour operating day. In the first stage, one day ahead of the operating day, we make decisions on the hourly binary unit commitment decisions, start-up and shut-down status of each thermal generator and the total gas supply quantity from wells, along with pressures at each gas node, gas flows in each pipeline and the gas compressor working schedule $x \equiv (u_{m,t}, v^u_{m,t}, v^d_{m,t}, p^{ng}_{\lambda}, \pi_{j,t}, \Delta\pi^k_{j,j'}, \eta_{j,j',t}, y^k_{j,j',t}, \delta^k_{j,j',t})$. These decisions are made in advance because of minimum up- and down-times, ramping constraints, and the time required for gas to travel through pipelines. Then, for each scenario time series of wind energy availability, the hourly dispatch solution of the power system, including energy production and transmission quantities, as well as storage levels and flows in and out of gas storage facilities, $z_s \equiv (p^{wind}_{w,t,s}, p_{m,t,s}, l_{\psi,t,s}, \mu_{g,t,s}, q^{in}_{\psi,t,s}, q^{out}_{\psi,t,s}, \theta_{i,t,s}, f_{i,i',t,s}, \alpha^-_{j,t,s}, \alpha^+_{j,t,s}, \beta^-_{j,t,s}, \beta^+_{j,t,s}, \gamma^-_{j,t,s}, \gamma^+_{j,t,s})$, are determined. Thus, the second stage represents the ISO's real time dispatch decisions and natural gas system's real time working pattern of the storage facilities. To focus on the uncertainty from wind energy, equipment outages are not considered. Wind generators are modeled as dispatchable to reflect day-ahead market practices such as those in the Midcontinent Independent System Operator (MISO) in the US, where they participate as Dispatchable Intermittent Resources [26]. The model is:

$$\begin{aligned}\zeta^{SP} = \min \; & \sum_{t\in\mathcal{T}} \Bigg\{ \sum_{n\in\mathcal{N}} \left(C^{su}_n v^u_{n,t} + C^{sd}_n v^d_{n,t}\right) + \sum_{g\in\mathcal{G}} \left(C^{su}_g v^u_{g,t} + C^{sd}_g v^d_{g,t}\right) + \sum_{\lambda\in\Lambda} C^{ng}_{\lambda} p^{ng}_{\lambda} \\ & + \sum_{s\in\mathcal{S}} \xi^s \Bigg[\sum_{n\in\mathcal{N}} C^{prod}_n p_{n,t,s} + \sum_{i\in\mathcal{I}} \left(\Gamma^+_{\beta}\beta^+_{i,t,s} + \Gamma^-_{\beta}\beta^-_{i,t,s}\right) + \sum_{j\in\mathcal{J}} \left(\Gamma^+_{\alpha}\alpha^+_{j,t,s} + \Gamma^-_{\alpha}\alpha^-_{j,t,s}\right) + \sum_{\psi\in\Psi} C^{stor}_{\psi} q^{out}_{\psi,t,s} \Bigg] \Bigg\} \end{aligned} \tag{1}$$

$$s.t. \sum_{j\in\mathcal{J}} \sum_{g\in\mathcal{G}(i,j)} p_{g,t,s} + \sum_{n\in\mathcal{N}(i)} p_{n,t,s} + \sum_{w\in\mathcal{W}(i)} p^{wind}_{w,t,s} + \sum_{i''\in\mathcal{I}''(i)} f_{i'',i,t,s} + \beta^-_{i,t,s} = D^e_{i,t} + \sum_{i'\in\mathcal{I}'(i)} f_{i,i',t,s} + \beta^+_{i,t,s}, \quad \forall i,t,s \tag{2}$$

$$u_{m,t} - u_{m,t-1} = v^u_{m,t} - v^d_{m,t-1}, \quad \forall m \in \mathcal{M}, t \tag{3}$$

$$u_{m,t} \geq v^u_{m,t}, \quad \forall m \in \mathcal{M}, t \tag{4}$$

$$u_{m,t} \leq 1 - v^d_{m,t}, \quad \forall m \in \mathcal{M}, t \tag{5}$$

$$v^u_{m,t} + v^d_{m,t} \leq 1, \quad \forall m \in \mathcal{M}, t \tag{6}$$

$$\sum_{tt=t-T^{on}_m+1}^{t} v^u_{m,tt} \leq u_{m,t}, \quad \forall m \in \mathcal{M}, i, t \tag{7}$$

$$\sum_{tt=t-T^{off}_m+1}^{t} v^d_{m,tt} \leq 1 - u_{m,t}, \quad \forall m \in \mathcal{M}, i, t \tag{8}$$

$$p_{m,t,s} \geq \underline{P}_m \left(u_{m,t} - v^u_{m,t}\right), \quad \forall m \in \mathcal{M}, t, s \tag{9}$$

$$p_{m,t,s} \leq \overline{P}_m \left(u_{m,t} - v^u_{m,t}\right) + \underline{P}_m \left(v^d_{m,t} + v^u_{m,t}\right), \quad \forall m \in \mathcal{M}, t, s \tag{10}$$

$$p^{wind}_{w,t,s} \leq \overline{P}^{wind}_{w,t,s}, \quad \forall w \in \mathcal{W}_i, i, t, s \tag{11}$$

$$-R^{down}_m \leq p_{m,t,s} - p_{m,t-1,s} \leq R^{up}_m, \quad \forall m \in \mathcal{M}, t, s \tag{12}$$

$$-\overline{F}_{i,i'} \leq f_{i,i',t,s} \leq \overline{F}_{i,i'}, \quad \forall i' \in \mathcal{I}'(i), i, t, s \tag{13}$$

$$f_{i,i',t,s} = \frac{\theta_{i,t,s} - \theta_{i',t,s}}{X_{i,i'}}, \quad \forall i' \in \mathcal{I}'(i), i, t, s \tag{14}$$

$$\mu_{g,t,s} = \phi_g p_{g,t,s}, \quad \forall g \in \mathcal{G}, t, s \tag{15}$$

$$\begin{aligned} &\alpha^-_{j,t,s} + \sum_{\lambda \in \Lambda(j)} \frac{p^{ng}_\lambda}{|\mathcal{T}|} + \sum_{\psi \in \Psi(j)} \left(q^{out}_{\psi,t,s} - q^{in}_{\psi,t,s}\right) + \sum_{j'' \in \mathcal{J}''(j)} \eta_{j'',j,t} + \sum_{c'' \in \mathcal{C}''(j)} \eta_{c'',j,t} \\ &\qquad = D^{ng}_{j,t} + \sum_{j' \in \mathcal{J}'(j)} \eta_{j,j',t} + \sum_{c' \in \mathcal{C}'(j)} \eta_{j,c',t} + \sum_{i \in \mathcal{I}} \sum_{g \in \mathcal{G}(i,j)} \mu_{g,t,s} + \alpha^+_{j,t,s}, \forall j, t, s \end{aligned} \tag{16}$$

$$\underline{L}_\psi \leq l_{\psi,t,s} \leq \overline{L}_\psi, \quad \forall \psi, t, s \tag{17}$$

$$-Q_\psi \leq \left(q^{out}_{\psi,t,s} - q^{in}_{\psi,t,s}\right) \leq Q_\psi, \quad \forall \psi, t, s \tag{18}$$

$$l_{\psi,t,s} = l_{\psi,t-1,s} - q^{out}_{\psi,t,s} + q^{in}_{\psi,t,s}, \quad \forall \psi, t, s \tag{19}$$

$$l_{\psi,t-1,s} - \overline{L}_\psi \leq q^{out}_{\psi,t,s} - q^{in}_{\psi,t,s} \leq l_{\psi,t-1,s} - \underline{L}_\psi, \quad \forall \psi, t, s \tag{20}$$

$$\underline{\pi}_j \leq \pi_{j,t} \leq \overline{\pi}_j, \quad \forall j, t \tag{21}$$

$$\frac{\pi_{j,t}}{\tau_{j,c'}} \leq \pi_{c',t} \leq \pi_{j,t}\tau_{j,c'}, \quad \forall c' \in \mathcal{C}'(j), t \tag{22}$$

$$\eta_{j,j',t} = sgn\left(\pi_{j,t} - \pi_{j',t}\right) C_{j,j'} \sqrt{|\pi_{j,t} - \pi_{j',t}|}, \quad \forall j' \in \mathcal{J}'(j), t \tag{23}$$

The objective (1) is to minimize the total expected cost which consists of the first stage cost, including

the thermal generator start-up and shut-down costs and gas supply cost (first line), and the second stage cost (second line), including the expected electricity production costs of non-gas-fired conventional generators, penalties on unserved/excess electricity, penalties on unserved/excess gas and the net cost of gas flows from storage. Here we count the power production costs for non-gas-fired generators as the product of the production cost per unit electricity and the electricity production. The production costs of the gas-fired generators are the fuel costs coming from the gas production or storage facilities. Constraints (2) represent the energy balance at each electricity node in each hour. The UC constraints (3)–(6) describe the connection between start-up/shut-down and unit on/off status variables. Constraints (7)–(8) enforce generator minimum on/off times. Constraints (9)–(10) describe upper and lower limits for the generator production levels and constraints (11) impose upper bounds on the wind energy output according to the available wind energy for each hour. Constraints (12) specify generator ramping limits. Constraints (13)–(14) represent the lossless, linearized DC formulation of power flows, limited by the transmission line capacities.

The gas and power system are connected through the amount of gas consumed by gas-fired generators (15).

The gas flow constraints (16) describe the flow conservation for each scenario in each hour at each node. Constraints (17)–(18) enforce upper and lower bounds on the storage levels and flow rates into and out of each gas storage facility. Constraints (19) connect storage levels of consecutive hours with the flow rates. Constraints (20) impose limits on the flow rates to maintain storage levels within prescribed bounds. Because the gas flow through a pipeline, as described by the Weymouth equation, depends on the difference of squared pressure levels between its two end nodes, the gas flow model is formulated in terms of these squared pressures, $\pi_{j,t}$, which are bounded by constraints (21). According to a simplified compressor model, the squared pressure increase ratio in each active pipeline is bounded as in (22) [27]. It limits the gas pressure increase ratio through compressors. The WEs (23) are applied to characterize the gas flows in passive pipelines.

According to the WEs, the gas flow in a passive pipeline is a continuous, nonlinear and non-convex function of the squared pressures at the two end nodes of the pipeline. An incremental method is applied to approximate the nonlinear constraints as piecewise linear with additional binary variables because it is the fastest and most accurate linearization method for the nonlinear Weymouth equation [21]. We divide the squared pressure range into segments and introduce a continuous variable δ^k and a binary variable y^k for each segment, k, where δ^k represents the portion of segment k that is used and the values of y^k ensure that if any part of a segment is used then all lower-valued segments must be completely used [28]. Upon dividing its domain into intervals with breakpoints $x^k, k \in \mathcal{K}$, a one-dimensional nonlinear function $h(x)$ can

be approximated as (24)–(28).

$$h\left(x\right) \approx h\left(x^{1}\right) + \sum_{k \in \mathcal{K}} \left[h\left(x^{k+1}\right) - h\left(x^{k}\right)\right] \delta^{k} \tag{24}$$

$$x = x^{1} + \sum_{k \in \mathcal{K}} \left(x^{k+1} - x^{k}\right) \delta_{k} \tag{25}$$

$$\delta^{k+1} \leq y^{k} \leq \delta^{k}, \quad \forall k \in \mathcal{K} - 1 \tag{26}$$

$$0 \leq \delta^{k} \leq 1, \quad \forall k \in \mathcal{K} \tag{27}$$

$$y^{k} \in \{0, 1\}, \quad \forall k \in \mathcal{K} \tag{28}$$

Accordingly, we linearize constraints (23) as (29)–(35), where the quantities $\Delta\pi^{k}_{j,j',t}$ are fixed constants.

$$\Delta\pi_{j,j',t} = \pi_{j,t} - \pi_{j',t}, \quad \forall j' \in J'(j), j, t \tag{29}$$

$$\Delta\pi_{j,j',t} = \Delta\pi^{1}_{j,j',t} + \sum_{k \in \mathcal{K}} \left(\Delta\pi^{k+1}_{j,j',t} - \Delta\pi^{k}_{j,j',t}\right) \delta^{k}_{j,j',t} \tag{30}$$

$$\eta_{j,j',t} = \eta^{1}_{j,j',t} + \sum_{k \in \mathcal{K}} \left(\eta^{k+1}_{j,j',t} - \eta^{k}_{j,j',t}\right) \delta^{k}_{j,j',t} \tag{31}$$

$$\eta^{k}_{j,j',t} = sgn\left(\Delta\pi^{k}_{j,j',t}\right) C_{j,j'} \sqrt{\left|\Delta\pi^{k}_{j,j',t}\right|} \tag{32}$$

$$\delta^{k+1}_{j,j'} \leq y^{k}_{j,j'} \leq \delta^{k}_{j,j'}, \quad \forall k \in \mathcal{K} - 1 \tag{33}$$

$$0 \leq \delta^{k}_{j,j'} \leq 1, \quad \forall k \in \mathcal{K} \tag{34}$$

$$y^{k}_{j,j'} \in \{0, 1\}, \quad \forall k \in \mathcal{K} \tag{35}$$

Overall, the SP model includes equations (1)–(22) and (29)–(35).

3.2 Deterministic Model with Reserves (DR)

The deterministic model with reserves has been implemented in the power system industry, but nobody implemented it for the integrated operation of the power and natural gas system operation. Here we incorporate a simple deterministic model with reserves as the comparable baseline for the SP model. The DR model includes constraints (2)–(9), (11), (13)–(22), and (29)–(35) with $\mathcal{S} = \{f\}, \xi_{f} = 1$ and $\overline{P}^{wind}_{w,t,f} = \hat{P}^{wind}_{w,t}, \forall w, t$. As in the traditional practice, day-ahead uncertainty in the wind energy is managed by including reserves. The objective function (36) includes an additional term for non-supplied/excess reserves, and the reserve

limits are imposed by replacing the dispatch constraints (10) and (12) with (37)–(40). Here we model only operating reserves, which are proportional to the hourly total wind energy forecast as described in (38), to protect against wind energy forecast errors. This is consistent with the SP model including scenarios for uncertain wind energy only. Both the SP and the DR models could be extended to include additional types of reserves including regulating, load-following, contingency, spinning and non-spinning reserves.

$$\begin{aligned}\min \quad & \sum_{t\in\mathcal{T}}\Bigg\{\sum_{n\in\mathcal{N}}\left(C_n^{su}v_{n,t}^{u}+C_n^{sd}v_{n,t}^{d}\right)+\sum_{g\in\mathcal{G}}\left(C_g^{su}v_{g,t}^{u}+C_g^{sd}v_{g,t}^{d}\right)+\sum_{\lambda\in\Lambda}C_\lambda^{ng}p_\lambda^{ng}+\sum_{n\in\mathcal{N}}C_n^{prod}p_{n,t,f}\\ &+\sum_{i\in\mathcal{I}}\left(\Gamma_\beta^{+}\beta_{i,t,f}^{+}+\Gamma_\beta^{-}\beta_{i,t,f}^{-}\right)+\sum_{j\in\mathcal{J}}\left(\Gamma_\alpha^{+}\alpha_{j,t,f}^{+}+\Gamma_\alpha^{-}\alpha_{j,t,f}^{-}\right)+\sum_{\psi\in\Psi}C_\psi^{stor}q_{\psi,t,f}^{out}+\Gamma_\gamma^{+}\gamma_{t,f}^{+}+\Gamma_\gamma^{-}\gamma_{t,f}^{-}\Bigg\}\end{aligned} \tag{36}$$

$$0\le p_{m,t,f}+r_{m,t,f}\le\overline{P}_m\left(u_{m,t}-v_{m,t}^{u}\right)+\underline{P}_m\left(v_{m,t}^{d}+v_{m,t}^{u}\right),\quad\forall m\in\mathcal{M},t \tag{37}$$

$$\sum_{m\in\mathcal{M}}r_{m,t,f}+\gamma_{t,f}^{-}-\gamma_{t,f}^{+}=WR\sum_{w\in\mathcal{W}}\hat{P}_{w,t}^{wind},\quad\forall t \tag{38}$$

$$-R_m^{down}\le p_{m,t,f}-p_{m,t-1,f},\quad\forall m\in\mathcal{M},t \tag{39}$$

$$p_{m,t,f}+r_{m,t,f}-p_{m,t-1,f}\le R_m^{up},\quad\forall m\in\mathcal{M},t \tag{40}$$

To test the performance of the day-ahead decisions made according to the DR model, we simulate real-time dispatch by fixing the day-ahead decisions and resolving the DR model for each wind energy scenario s in the original set S while replacing f by s in equations (36)–(40) and setting $r_{m,t,s}=\gamma_{t,s}^{+}=\gamma_{t,s}^{-}=0,\forall m\in\mathcal{M},t,s$. Denoting the optimal cost of the solution under scenario s by ζ_s^{DR}, the expected cost of the DR day-ahead decisions is given by $\zeta^{DR}=\sum_{s\in\mathcal{S}}\xi_s\zeta_s^{DR}$. Fig. 1 depicts the process for comparing the SP model with the DR model.

3.3 Lower Bound for Model Evaluation

A lower bound on the optimal cost from both models can be found by supposing it were possible to make day-ahead decisions with perfect knowledge of the wind energy. We refer to this as the wait and see (WS) model (41) . In the WS model, the decision maker makes no decisions until all random parameters $\overline{P}_{w,t,s}^{wind}$ are realized. The optimal values of all decision variables and the objective are scenario-dependent. Denoting the optimal objective value for scenario s as ζ_s^{WS}, the optimal objective value of the WS model is $\Sigma\xi_s\zeta_s^{WS}\le$

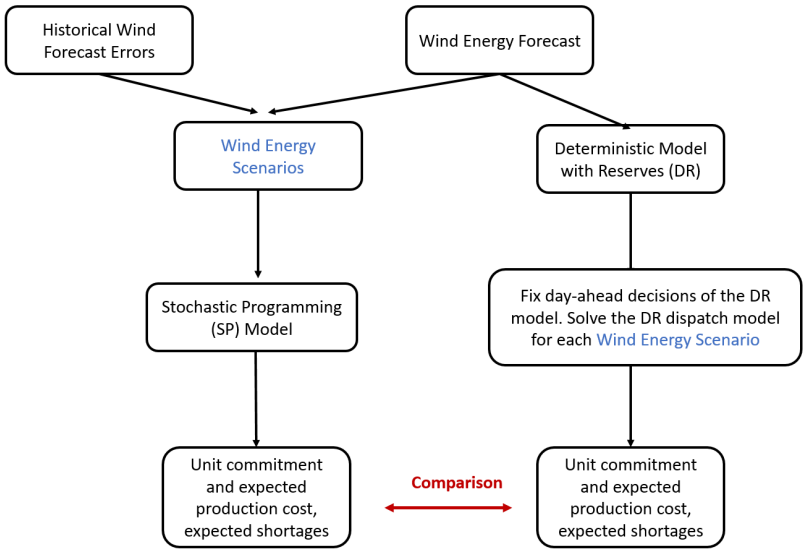

Figure 1: Flowchart of procedure for comparing the stochastic programming model and the deterministic model with reserves.

$\zeta^{SP} \leq \zeta^{DR}$.

$$\begin{aligned}\zeta_s^{WS} = \min \Bigg\{ & \sum_{t\in\mathcal{T}} \Bigg[\sum_{n\in\mathcal{N}} \left(C_n^{su} v_{n,t}^u + C_n^{sd} v_{n,t}^d\right) + \sum_{g\in\mathcal{G}} \left(C_g^{su} v_{g,t}^u + C_g^{sd} v_{g,t}^d\right) + \sum_{\lambda\in\Lambda} C_\lambda^{ng} p_\lambda^{ng} \\ & + \sum_{n\in\mathcal{N}} C_n^{prod} p_{n,t,s} + \sum_{i\in\mathcal{I}} \left(\Gamma_\beta^+ \beta_{i,t,s}^+ + \Gamma_\beta^- \beta_{i,t,s}^-\right) + \sum_{j\in\mathcal{J}} \left(\Gamma_\alpha^+ \alpha_{j,t,s}^+ + \Gamma_\alpha^- \alpha_{j,t,s}^-\right) + \sum_{\gamma\in\Psi} C_\psi^{stor} q_{\psi,t,s}^{out} \Bigg] \\ & : (2) - (8), \\ & (9) - (22), (29) - (35) \quad \text{enforced for this } s \text{ only} \Bigg\}\end{aligned} \tag{41}$$

4 Numerical Studies

We apply our models in two case studies consisting of a six-bus power system with a seven-node gas system [5] and the IEEE 24-bus system with a 20-node gas system. The purpose of the first case study is to compare the total cost distributions of the WS, SP and DR models. The second case study is used to find the scheduling differences of the SP and DR models and compare the resulting risks and costs. We use a common set of wind energy scenarios, scaled to the wind capacity, in both cases. Because the wind energy scenarios depend on the uncertainty in the wind forecast and this uncertainty varies from day to day, we assess the performance in multiple days in each case study. We assume that 1 kcf of natural gas can generate 1 MBtu of energy in both cases. The mixed-integer programs are solved in their extensive form with GAMS/CPLEX 23.4.3 on a Linux workstation (40 CPU, 252GB RAM).

4.1 Scenario Generation

Various methods have been proposed for generating wind power scenarios. As this task is not the focus of this paper, we employ wind power scenarios generated for stochastic UC according to the approach described by [29, 30] and assessed by [31]. The important features of this approach are that it identifies a segment of similar historical days based on the characteristics of the day-ahead wind power forecast trajectory and then approximates the stochastic process for actual wind energy within that segment by conditional expectations within ranges of the forecast error distributions for different hours. As a result, a specified number of unequally likely scenario trajectories are generated with different amounts of dispersion on different days. This method can be extended to generate wind energy scenarios with whatever level of temporal detail is available in the forecast and actual wind data. For more details of the scenario generation process, please see [30]. Wind forecast data were obtained from the Bonneville Power Administration [32, 33]. The observed data and the wind generation capacity are available from [33] and [34], respectively. Data were collected for a recent year but, due to missing information for some days, scenarios were generated for only 340 days. A set of 27 scenarios was used for each day with probabilities ranging from 0.0001 to 0.5845. They were scaled according to specified wind capacity penetrations in each case study. To avoid end-of-study effects, the scheduling problems were solved over a 36-hour horizon. Deterministic loads for the first twelve hours were repeated to represent hours 25-36, while each wind power scenario was concatenated with the corresponding one for the following day.

4.2 Six-Bus system

The six-bus power system with seven-node gas system has two NGPGs, one coal fueled generator, one wind generator (farm), three power loads, seven transmission lines, one storage facility, one active pipeline, five passive pipelines, two non-electric gas loads and two gas suppliers [5], as shown in Fig. 1. Hourly gross non-electric gas demand is 6000 kcf/h, divided between gas nodes 2 and 4 with the ratio of 2 to 1. The electric load is divided among power nodes 1, 2 and 3 with the ratio of 1:2:2. We set the hourly reserve margin for wind power WR to be 5% [35]. The wind generation capacity is 20% of the total thermal capacity. The start-up and shut-down cost of all the generators are zero for this case study. All the data are available at [39].

Let $x_{d,s}^{MM}$ and $z_{d,s}^{MM}$ denote the optimal values of the first-stage variables and second-stage variables in scenario s from model MM for day d, respectively $MM \in \{DR, SP, WS\}$. The first-stage variables $x_{d,s}^{MM}, MM \in \{SP, DR\}$ are the same for all scenarios s; i.e., nonanticipative. Although the optimization process minimizes the total cost over 36 hours, only the optimal decisions of the 24 hours would be imple-

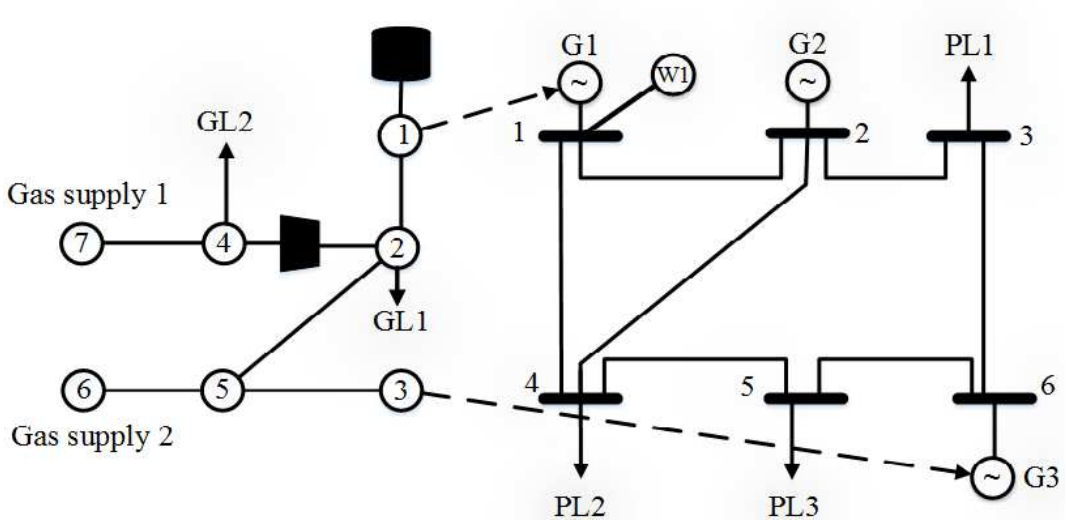

Figure 2: Six-bus power system with seven-node gas system. The natural gas system with gas loads (GL) shown on the left-hand side and the power system with power loads (PL), generators (G) and wind generators (W) is shown on the right-hand side. Dashed lines show connections between the two systems.

mented. Let $f(x, z)$ denote the 24-hour cost. Expressions (42)–(43) define the daily expected cost and the cost standard deviation which are used to evaluate the expected total cost and the proxy measure of risk since it is mostly driven by the unserved energy penalties for model MM. The mean expected cost and mean cost standard deviation for $|D|$=340 days are found by using equations (44)–(46).

$$E_d^{MM} = \sum_{s \in S} \xi_s f(x_{d,s}^{MM}, z_{d,s}^{MM}) \tag{42}$$

$$\sigma_d^{MM} = \sqrt{\sum_{s \in S} \xi_s \left[f(x_{d,s}^{MM}, z_{d,s}^{MM}) - E_d^{MM} \right]^2} \tag{43}$$

$$\overline{E^{WS}} = \frac{1}{|D|} \sum_{d=1}^{|D|} E_d^{WS}, \overline{\sigma^{WS}} = \frac{1}{|D|} \sum_{d=1}^{|D|} \sigma_d^{WS} \tag{44}$$

$$\overline{E^{SP}} = \frac{1}{|D|} \sum_{d=1}^{|D|} E_d^{WS}, \overline{\sigma^{SP}} = \frac{1}{|D|} \sum_{d=1}^{|D|} \sigma_d^{SP} \tag{45}$$

$$\overline{E^{DR}} = \frac{1}{|D|} \sum_{d=1}^{|D|} E_d^{WS}, \overline{\sigma^{DR}} = \frac{1}{|D|} \sum_{d=1}^{|D|} \sigma_d^{DR} \tag{46}$$

Based on experimentation described in Section 4.3, we approximate the nonlinear functions with 20 piecewise linear segments. A similar approximation accuracy experiment is conducted in [36] based on Taylor series expansion to linearize the nonlinear constraints. Table 1 illustrates that the SP model has mean expected cost and standard deviation nearly as low as the WS model. The DR model results in 36%

higher mean expected cost and 32% higher mean standard deviation than the SP model. Fig. 3 shows the relative frequency distributions for expected cost and cost standard deviation for the first 24 hours. Because the high cost values are driven by the penalties for unserved energy, we can conclude that the SP model makes more reliable decisions given different wind uncertainty.

Table 1: Mean expected cost and standard deviation comparison over 36 hours as well as the first 24 hours.

	Mean expected cost, $\overline{E^{MM}}$ ($)		Mean standard deviation, $\overline{\sigma^{WS}}$ ($)	
MM	36 hours	24 hours	36 hours	24 hours
WS	670,351	456,755	3,819	2,737
SP	674,114	459,331	3,847	2,883
DR	886,309	623,264	5,168	3,514

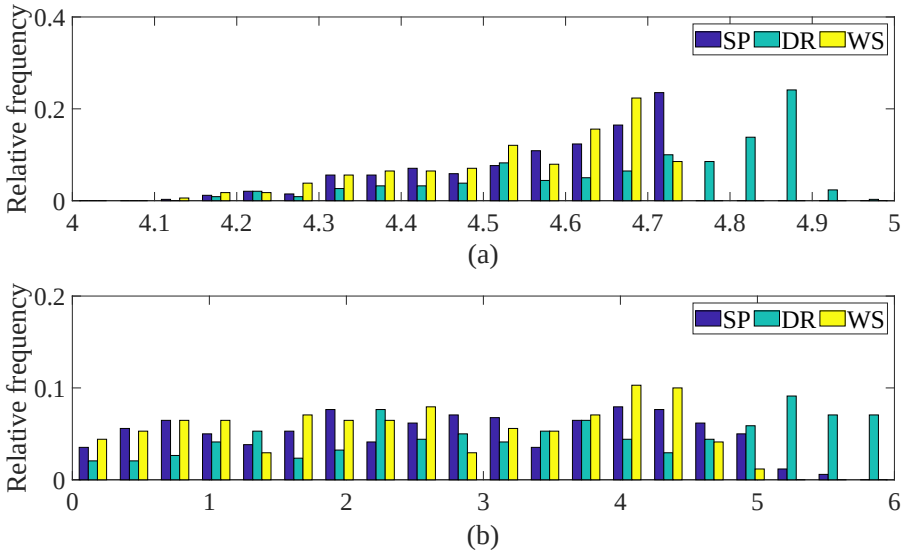

Figure 3: (a) Distribution of first 24 hour expected cost E_d ($\$10^5$); (b) Distribution of first 24 hour cost standard deviation σ_d ($\$10^3$).

4.3 24-Bus System

A modified IEEE 24-bus system and modified Belgian 20-node natural gas system are used according to [27] as shown in Fig. 4 with the ramp up and down rates and production cost revised in accordance with [37]. The system has 3 NGPGs, 4 coal-fired units, 3 hydro units, 2 wind generators, 38 transmission lines, 9 power loads, 2 gas suppliers (wells), 4 storage facilities, 21 passive pipelines, 3 active pipelines and 17 non-electric gas demands. The unserved energy and non-supplied reserves penalty cost are set to be $3500/MWh and $1100/MWh, respectively, as recommended by MISO [26]. The excess energy and reserve penalties are set

to be \$350/MWh and \$110/MWh, respectively, while the unserved gas and excess gas penalties are set to be \$3500/kcf and \$350/kcf, respectively. Fig. 5 shows the electric load and gas load of 36 hours in which the electric peak load occurs at hour 18 and gas peak load occurs at hour 9. The total thermal generating capacity is 3453 MW, which is the sum of the capacities of all the thermal generators in the IEEE 24-bus system. Two wind generators with identical capacity are added at nodes 7 and 15. Energy production by these wind generators is uncertain in advance. All the data are available at [39]. To compare the SP model and the DR model representing different levels of wind energy penetration and resulting uncertainty, we define the wind energy capacity penetration factor (WPF) to be the ratio of the total wind generation capacity to the total thermal generation capacity; i.e., WPF $= \frac{\sum_{w\in\mathcal{W}} \overline{P}_w^{wind}}{\sum_{m\in\mathcal{M}} \overline{P}_m}$. For example, given WPF=30%, the total wind energy capacity is $0.3 \times 3453\text{MW} = 1035.9\text{MW}$. This implies that each of the two wind generators has a capacity of 517.95 MW. As the WPF increases, the amount of uncertainty increases also; i.e., the variation of wind energy uncertainty given WPF=30% is six times that given WPF=5%.

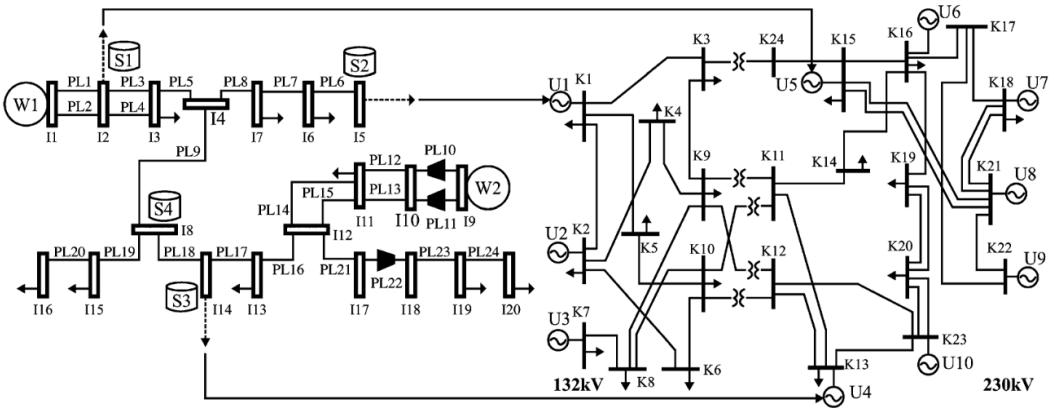

Figure 4: Modified IEEE 24-bus system and modified Belgian 20-node natural gas system [27]

We identify specific days to examine the results according to the dispersion of the scenarios. Because unserved energy is penalized at a higher rate than excess energy, we measure the dispersion according to the amount of positive deviation, or *discrepancy*, of a scenario from the forecast. Define ϵ_s to be the discrepancy between the wind energy forecast and scenario s.

$$\epsilon_s = \sum_{t=1}^{36} \sum_{w\in\mathcal{W}} \max\left\{\hat{P}_{w,t}^{wind} - \overline{P}_{w,t,s}^{wind}, 0\right\} \tag{47}$$

Fig. 6 shows the discrepancy histograms of four days, selected based on diversity in the expected value and variance of the discrepancy. Fig. 7 shows the wind scenarios and forecast distribution of these four days.

Day (a): Low expected discrepancy and low variance.

Day (b): Low expected discrepancy and medium variance.

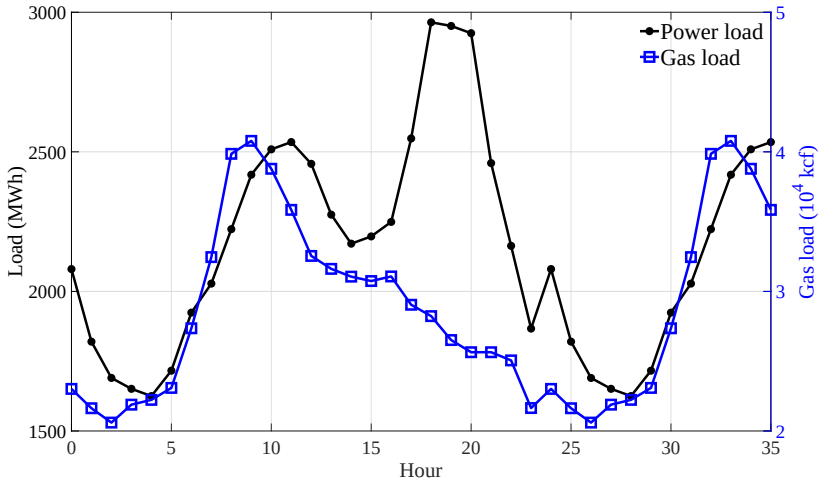

Figure 5: Power and gas load profiles.

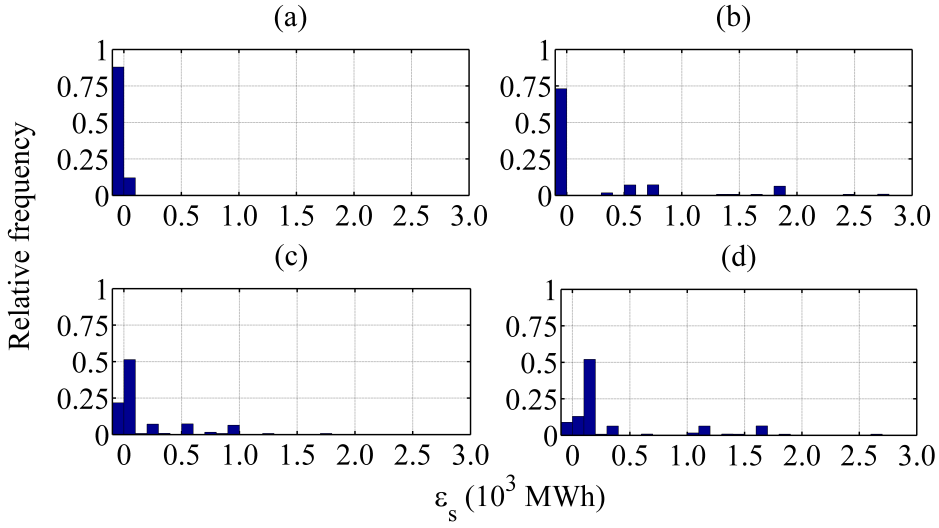

Figure 6: Discrepancy histogram of four days.

Day (c): Medium expected discrepancy and medium variance.

Day (d): Large expected discrepancy and large variance.

Before we compare the simulation results of the SP and DR models, we conduct an experiment to study the effect of the number of linearization segments $|K|$ for both models for day (d) to choose an efficient approximation while maintaining a relatively accurate cost. Each segment has equal length. The minimum and maximum breakpoints of a passive pipeline from j to j' are $\underline{\pi}_j - \overline{\pi}_{j'}$ and $\overline{\pi}_j - \underline{\pi}_{j'}$, respectively. As illustrated in Tables 2 and 3, as $|K|$ increases from 2 to 80, the optimal costs of SP and DR model first change rapidly and become stable when $|K| \geq 40$, while the computational time generally increases with $|K|$. In addition, it takes more than 24 hours to find the optimal solution when $|K| = 80$. Because the daily short-term operation of natural gas and power system requires solutions to be found quickly, we choose

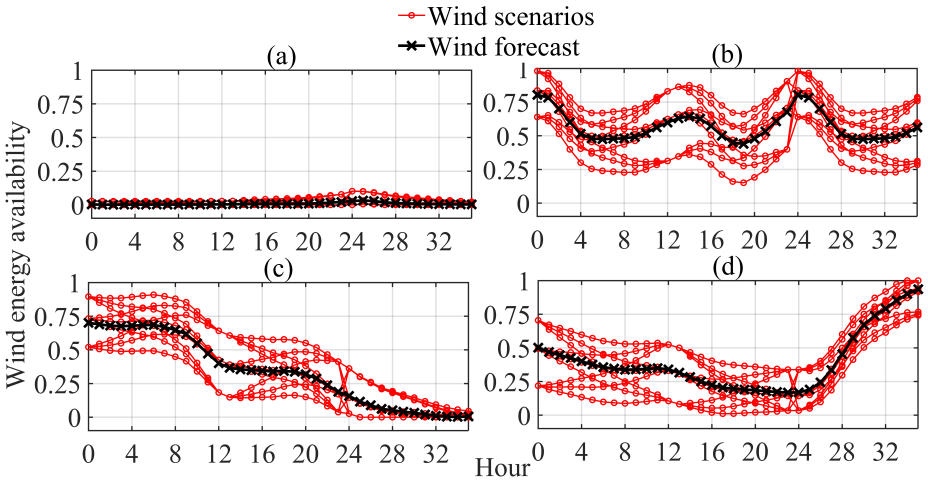

Figure 7: Hourly wind availability of scenarios and forecast for four selected days, scaled as a fraction of capacity.

Table 2: SP model segment experiment result for day (d)

	WPF=5%						WPF=15%						WPF=30%					
$\|K\|$	2	5	10	20	40	80	2	5	10	20	40	80	2	5	10	20	40	80
Expected Cost (10^3\$)	1,822	1,782	1,782	1,782	1,782	1,782	1,741	1,701	1,701	1,701	1,701	1,701	1,649	1,609	1,609	1,609	1,609	1,609
Time (10^3s)	10.3	0.7	5.5	42.6	18.6	143.6	7.5	1.5	0.5	0.5	0.8	94.3	6.5	1.6	55.3	44.7	59.7	77.8

$|K|= 40$ for the following case study.

To compare the costs and risks from the SP and DR models, we plot the UC and expected production cost versus expected shortage across all 27 scenarios for the first 24 hours with WPF of 5%, 15% and 30% and WR of 10%, 20%, 30%, 40%, 50%, 60%, 70%, 80%, 90% and 100% in Fig. 8. The rows and columns contain plots for different cases and WPF levels, respectively. The SP model has no unserved energy in any of the 12 subplots. As the WPF increases from 5% to 30%, the 24-hour UC and expected production cost decreases for all four of the days and both models. The DR model has zero unserved energy and lower 24-hour UC and expected cost than the SP model given WPF equals to 5%. Here we minimize the expected cost including not only UC and expected production cost but also unserved and excess penalties for 36 hours. It is not guaranteed that the first 24-hour UC and expected cost of the SP model is less than that of the DR model. For each of the four cases, the SP model has less expected shortage than the DR model when the WPF equals 15% or 30%, indicating that the SP model lowers the risk of operating the system while maintaining a low UC and expected production cost.

Day (b) has the largest difference between the SP and DR models, as illustrated in Fig. 6(b). As the WPF increases to 30%, the expected energy shortage of the DR model increases dramatically while that of the SP model remains at zero. In addition, as the WR increases from 10% to 100%, the expected shortage of

Table 3: DR model segment experiment result for day (d)

		WPF=5%						WPF=15%						WPF=30%					
	$\|K\|$	2	5	10	20	40	80	2	5	10	20	40	80	2	5	10	20	40	80
	WR																		
Expected Cost (10^3\$)	0.1	1822	1782	1782	1790	1782	1782	1742	1728	1720	1720	1728	1728	1656	1622	1622	1622	1622	1622
	0.2	1822	1790	1790	1782	1790	1782	1765	1728	1741	1720	1741	1741	1658	1624	1624	1624	1624	1624
	0.3	1822	1782	1782	1782	1790	1782	1765	1728	1728	1741	1720	1728	1665	1630	1631	1630	1631	1630
	0.4	1822	1782	1782	1790	1782	1790	1765	1728	1720	1741	1728	1728	1668	1634	1634	1634	1634	1634
	0.5	1822	1782	1790	1790	1782	1782	1747	1708	1708	1708	1708	1708	1677	1628	1628	1628	1628	1628
	0.6	1831	1786	1786	1786	1786	1794	1747	1708	1708	1708	1708	1708	1670	1630	1630	1631	1630	1632
	0.7	1831	1782	1787	1782	1787	1787	1749	1708	1708	1708	1708	1708	1672	1632	1632	1632	1632	1632
	0.8	1831	1787	1787	1782	1782	1782	1749	1710	1710	1710	1710	1710	1683	1642	1642	1642	1642	1642
	0.9	1822	1787	1782	1782	1782	1782	1750	1711	1711	1711	1711	1711	1691	1644	1644	1644	1644	1644
	1	1822	1787	1782	1787	1787	1787	1757	1719	1719	1718	1719	1719	1698	1652	1654	1652	1652	1654
Total Time ($10^3 s$)		1.21	1.87	2.89	4.95	9.93	27.32	1.32	1.61	2.51	4.95	12.84	22.72	1.32	1.84	2.94	5.54	12.77	231.61

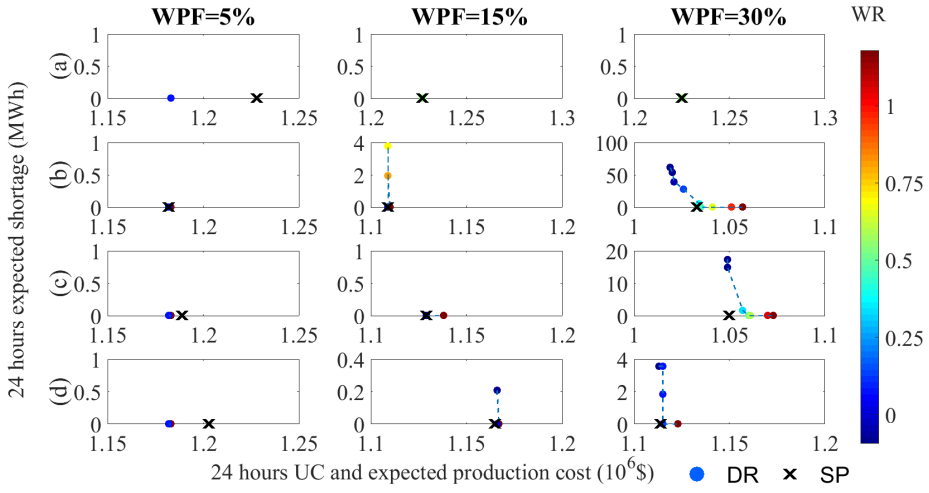

Figure 8: Expected total cost less penalty versus expected shortage of the first 24 hours with WPF of 5%, 15% and 30% and WR ranging from 10% to 100%. The scale of each subplot is adjusted for visibility of the results and the comparison between the DR model and the SP model within each subplot.

the DR model decreases. When WR is greater than 80%, there is no unserved energy in the DR model, and the UC and expected production cost of the SP model is less than that of the DR model. Table 4 displays the hourly UC schedule for day (b) with WPF of 30%, selected based on the greatest difference between the results of the two models, and WR of 40%. Among the seven thermal units, units 1, 4 and 5 are NGPGs, while units 2, 3, 6 and 7 are coal fueled. Units 8, 9 and 10 are hydro generators which are assumed free and always on. Here the NGPGs are cheaper than the coal fueled generators and the SP model always commits one unit more than the DR model does in hour 7–21. Production levels of well 1 of the SP and DR models are identical and equal to 861,983 kcf/day, while those of well 2 are 0 kcf/day for both models. The corresponding 24 hour UC and expected production costs are \$1,032,629 and \$1,025,947, respectively, for the SP and DR models, while the respective expected shortage amounts are 0 and 28 MWh. The SP model commits more units in each hour to increase the committed capacity and assure that sufficient electricity can be produced in case less wind energy is available than forecast. The SP model is able to firm the variable wind energy

Table 4: Optimal unit commitment decisions for day (b) with WPF = 30% and WR = 40%.

Unit	Fuel Type	SP model hours (1-24)																							
1	Gas	1	1	1	1	1	1	0	0	0	0	1	1	1	1	1	1	1	1	1	1	1	1	1	1
4	Gas	1	1	1	1	1	1	1	1	1	1	1	1	1	1	1	1	1	1	1	1	1	1	1	1
5	Gas	1	1	1	1	1	1	1	1	0	0	0	0	1	1	1	1	1	1	1	1	1	1	1	1
2	Coal	0	0	0	0	0	0	0	1	1	1	1	1	1	1	1	1	1	1	1	1	1	0	0	0
3	Coal	1	1	1	1	1	1	1	1	1	1	1	1	1	1	1	1	1	1	1	1	1	1	1	1
6	Coal	0	0	0	0	0	0	0	0	0	0	0	0	0	0	0	0	0	0	0	0	0	0	0	0
7	Coal	1	1	1	1	1	1	1	1	1	1	1	1	1	0	0	0	0	0	0	0	0	0	0	0
Unit	**Fuel Type**	**DR model hours (1-24)**																							
1	Gas	1	1	1	1	1	1	1	1	1	1	1	1	1	1	1	1	1	1	1	1	1	1	1	1
4	Gas	1	1	1	1	1	1	1	1	1	1	1	1	1	1	1	1	1	1	0	0	0	0	0	0
5	Gas	1	1	1	1	1	1	1	0	0	0	0	0	0	0	0	0	0	1	1	1	1	1	1	1
2	Coal	0	0	0	0	0	0	0	0	0	0	0	0	0	0	0	0	0	0	0	0	0	0	0	0
3	Coal	1	1	1	1	1	1	1	1	1	1	1	1	1	1	1	1	1	1	1	1	1	1	1	1
6	Coal	0	0	0	0	0	0	0	0	0	0	0	0	0	0	0	0	0	0	0	0	0	0	0	0
7	Coal	1	1	1	1	1	1	1	1	1	1	1	1	1	1	1	1	1	1	1	1	1	0	0	0

by committing more units and supplying more gas since DR model makes the day-ahead decisions only on the basis of the wind energy forecast and reserve margins.

Table 5: Comparison of shortages in the first 24 hours for different scenarios day (b) with 30% wind capacity penetration factor (WPF) and 40% wind reserve margin (WR).

Scenario	1	2	3	4	5	6	7	8	9
Probability	0.0010	0.0079	0.0010	0.0079	0.0634	0.0080	0.0010	0.0080	0.0010
SP shortage	20	0	0	0	0	0	0	0	0
DR shortage	344	327	327	0	0	0	0	0	0
Scenario	10	11	12	13	14	15	16	17	18
Probability	0.0079	0.0636	0.0080	0.0636	0.5110	0.0647	0.0080	0.0646	0.0082
SP shortage	0	0	0	0	0	0	0	0	0
DR shortage	293	276	276	0	0	0	0	0	0
Scenario	19	20	21	22	23	24	25	26	27
Probability	0.0010	0.0080	0.0010	0.0080	0.0647	0.0082	0.0010	0.0082	0.0010
SP shortage	0	0	0	0	0	0	0	0	0
DR shortage	155	239	239	0	0	0	0	0	0

C

To explore the reliability comparison further, Table 5 reports shortages in different scenarios from using the SP and DR models in day (b) with 30% wind capacity penetration and 40% WR, reported for the first 24 hours. Scenario 1 has one of the most different shortage between the SP and DR models, where the shortages of the two models are 20 MWh and 344 MWh, respectively. Fig. 9 shows the wind energy availability time series of the scenarios 1, 10 and 19 as well as forecast for day (b), expanded from Fig. 7(b). In hour 20, the wind energy availability of scenario 1 is only 21% less than forecast, whereas at hour 1, the wind energy availability of scenario 1 is 80% less than forecast. On average the wind energy availability of scenario 1 is

55% of the forecast. The DR model resorts to 327 MW of electric load shedding in scenario 1 during hours 11–13 because of the high electric and gas loads and large wind energy discrepancy. A WR of 40% still results in considerable shortage because all four storage facilities run out of gas as listed in Fig. 10 and line congestion occurs. Specifically, for example, under scenario 1, power node 17 has the most non-served energy of 196.60 MWh in hour 12. There are three lines connecting to power node 17. Both line 28 from power node 16 to 17 and line 29 from power node 17 to 18 reach the maximum flow of -500 MWh. Line 31 from power nodes 17 to 22 has a flow of 196.60 MWh. In other words, among all the three lines connecting to power node 17, the optimal solution has only one power flow into power node 17 through line 29 and both the other two lines have power flows out of power node 17. Power flow constraints through line 29 are binding and congestion occurs. As the WR increases to 50%, the 24 hour expected unserved energy is reduced to 6 MWh and the UC and expected production cost increases to $\$1.035 \times 10^6$, whereas the cost of the SP model is $\$1.026 \times 10^6$. In general, the SP model is able to make day-ahead and real time decisions with a better cost-risk trade-off for the integrated natural gas and power system while accounting for network constraints, including crucial limitations on gas storage capacity, as well as the uncertain discrepancy between actual and forecast wind energy.

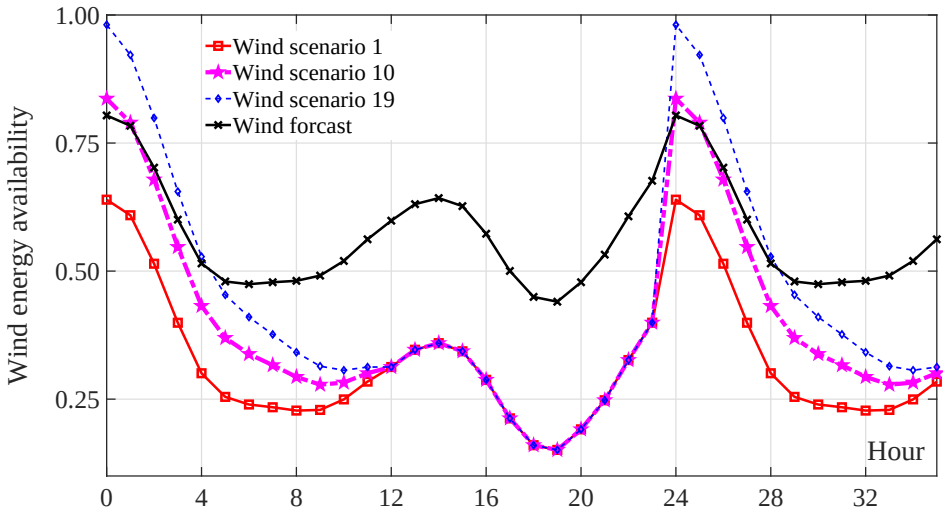

Figure 9: Hourly wind availability, scaled to capacity, of scenarios and forecast for day (b).

5 Conclusions

We compare a two-stage stochastic program (SP) and a deterministic model with forecast-based wind reserves (DR) to model the short-term combined scheduling of the natural gas and power systems while minimizing the total operational cost with uncertain wind energy. Simulation results are compared with multiple wind

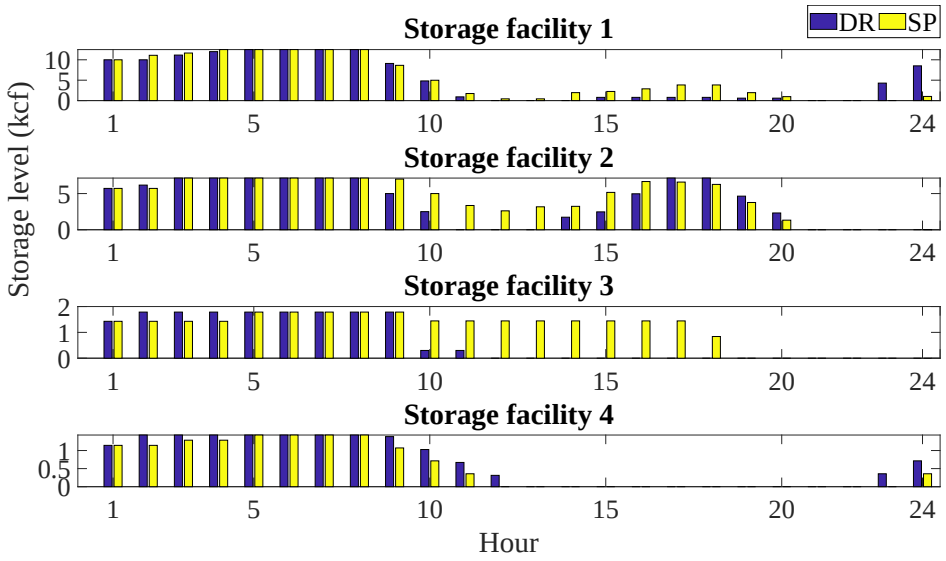

Figure 10: Hourly storage level of four storage facilities with 30% wind capacity penetration factor and 40% wind reserve margin for day (b) for scenario 1.

uncertainty scenarios in two case studies. In the smaller case study of a six-bus power system and seven-node natural gas system, we simulate a year's worth of days to capture the variability of the daily wind energy forecast and the resulting wind energy scenarios. The simulation results indicate that the SP model yields a much lower standard deviation and mean cost, suggesting that probabilistic-scenario-based scheduling of the combined system is better able to maintain a stable cost.

The two models are further compared using a 24-bus power system and 20-node natural gas system in four days that differ according to discrepancy between the wind energy scenarios and forecast, three WPF of 5%, 15% and 30%, and various wind reserve margins (WR). With WPF=5%, the DR model maintains no expected unserved energy and has less expected cost than the SP model. When the WPF equals 15% or 30%, the combination of expected cost and expected unserved energy resulting from the SP model consistently dominates that from the DR model. By adjusting the thermal unit commitments along with the gas supply and pipeline working schedule on the day ahead to the level of uncertainty present in the scenarios, the SP model avoids shortages (high risks) while achieving low costs given relatively high wind penetration level.

Linearization experiments were done for both the small and large case studies to choose a number of segments that balances accuracy and computational efficiency. The details of the large system segment experiment indicates that the SP model is more robust to the number of segments. In this paper we modeled the unit commitment and economic dispatch process of the power system in two stages. Alternatively, more stages may be included with, for example, a third stage that explicitly addresses the intra-hourly dispatch process. Security constraints could be added to protect against equipment failure. Finally, more efficient

stochastic programming solution algorithms such as progressive hedging could be applied to improve time and memory efficiency.

In future work, investigation of a good method to choose breakpoints in the piecewise linear formulation can improve approximation accuracy. To improve computational efficiency, use of the three-binary model [38] for unit commitment should be investigated also.

Acknowledgement

This material is based on work supported by Sandia National Laboratories.

References

[1] U. S. Department of Energy Information Administration: 'Annual energy outlook 2015 with projections to 2040', *US Department of Energy, Washington*, 2015, Available from: https://www.eia.gov/outlooks/aeo/pdf/0383(2015).pdf

[2] Shahidehpour, M., Fu, Y., Wiedman, T.: 'Impact of natural gas infrastructure on electric power systems', *Proc IEEE*, 2005, 93 **No. 5**, pp. 1042–1056

[3] Unsihuay, C., Marangon-Lima, J.W., de Souza, A.C.Z. 'Short-term operation planning of integrated hydrothermal and natural gas systems'. In: Proc. IEEE Lausanne Power Tech., 2007. pp. 1410–1416

[4] Li, T., Eremia, M., Shahidehpour, M.: 'Interdependency of natural gas network and power system security', *IEEE Trans. Power Syst.*, 2008, 23 **No. 4**, pp. 1817–1824

[5] Liu, C., Shahidehpour, M., Fu, Y., Li, Z.: 'Security-constrained unit commitment with natural gas transmission constraints', *IEEE Trans. Power Syst.*, 2009, 24 **No. 3**, pp. 1523–1536

[6] Liu, C., Shahidehpour, M., Wang, J.: 'Coordinated scheduling of electricity and natural gas infrastructures with a transient model for natural gas flow', *Chaos: Interdisc. J. Nonlinear Sci.*, 2011, 21 **No. 2**, pp. 25102

[7] Zhang, X., Shahidehpour, M., Alabdulwahab, A., Abusorrah, A.: 'Hourly electricity demand response in the stochastic day-ahead scheduling of coordinated electricity and natural gas networks', *IEEE Trans. Power Syst.*, 2016, 31 **No. 1**, pp. 592–601

[8] Correa-Posada, C.M., Sánchez-Martín, P. 'Stochastic contingency analysis for the unit commitment with natural gas constraints'. In: 2013 IEEE Grenoble Power Tech Conference. Grenoble, France, 2013, pp. 1–6

[9] Correa-Posada, C.M., Sánchez-Martín, P.: 'Security-constrained optimal power and natural-gas flow', *IEEE Trans. Power Syst.*, 2014, 29 **No. 4**, pp. 1780–1787

[10] Wen, Y., Qu, X., Li, W., Liu, X., Ye, X.: 'Synergistic operation of electricity and natural gas networks via ADMM', *IEEE Trans. Smart Grid*, 2018, 9 **No. 5**, pp. 4555–4565

[11] Biskas, P.N., Kanelakis, N.G., Papamatthaiou, A., Alexandridis, I.: 'Coupled optimization of electricity and natural gas systems using augmented Lagrangian and an alternating minimization method', *Int. J. of Elec. Power Energy Syst.*, 2016, 80, pp. 202–218

[12] Chen, S., Wei, Z., Sun, G., Wang, D., Zang, H.: 'Steady state and transient simulation for electricity-gas integrated energy systems by using convex optimisation', *IET Gener., Transm. Distrib.*, 2018, 12 **No. 9**, pp. 2199–2206

[13] Ge, S., Liu, X., Liu, H., Gu, C., Ge, L.: 'Research on unit commitment optimization of high permeability wind power generation and P2G', *Journal of Renewable and Sustainable Energy*, 2018, 10 **No. 3**, pp. 34702

[14] Jin, X., Mu, Y., Jia, H., Wu, J., Xu, X., Yu, X.: 'Optimal day-ahead scheduling of integrated urban energy systems', *Appl. Energy*, 2016, 180, pp. 1–13

[15] Khani, H., El-Taweel, N., Farag, H.E.Z.: 'Real-time optimal management of reverse power flow in integrated power and gas distribution grids under large renewable power penetration', *IET Gener., Transm. Distrib.*, 2018, 12 **No. 10**, pp. 2325–2331

[16] Li, Y., Zou, Y., Tan, Y., Cao, Y., Liu, X., Shahidehpour, M., et al.: 'Optimal stochastic operation of integrated low-carbon electric power, natural gas, and heat delivery system', *IEEE Trans. Sust. Energy*, 2018, 9 **No. 1**, pp. 273–283

[17] Xiao, X., Shui, Y., Gao, H., Liu, J., Chen, Q., Li, T., et al.: 'A two-stage distributionally robust coordinated dispatch for integrated electricity and natural-gas energy systems considering uncertainty of wind power', *IOP Conference Series: Materials Science and Engineering*, 2018, 366, pp. 012016. Available from: http://stacks.iop.org/1757-899X/366/i=1/a=012016?key=crossref.11ada094740d38017ce065073cf6efbb

[18] Osiadacz, A.: 'Simulation and analysis of gas networks'. (Gulf Publishing Company, Houston, TX, 1987)

[19] Thorley, A.R.D., Tiley, C.H.: 'Unsteady and transient flow of compressible fluids in pipelinesa review of theoretical and some experimental studies', *Int. J. Heat Fluid Fl.*, 1987, 8 **No. 1**, pp. 3–15

[20] Chaczykowski, M.: 'Transient flow in natural gas pipeline–The effect of pipeline thermal model', *Appl. Math. Model*, 2010, 34 **No. 4**, pp. 1051–1067

[21] Correa-Posada, C.M., Sánchez-Martín, P.: 'Gas network optimization: A comparison of piecewise linear models', *Optimization Online*, 2014,

[22] Wang, C., Wei, W., Wang, J., Bai, L., Liang, Y.: 'Distributed optimal gas-power flow using convex optimization and ADMM', *arXiv preprint arXiv:161004681*, 2016,

[23] He, C., Wu, L., Liu, T., Shahidehpour, M.: 'Robust co-optimization scheduling of electricity and natural gas systems via ADMM', *IEEE Trans. Sust. Energy*, 2017, 8 **No. 2**, pp. 658–670

[24] Alabdulwahab, A., Abusorrah, A., Zhang, X., Shahidehpour, M.: 'Coordination of interdependent natural gas and electricity infrastructures for firming the variability of wind energy in stochastic day-ahead scheduling', *IEEE Trans. Sust. Energy*, 2015, 6 **No. 2**, pp. 606–615

[25] Qadrdan, M., Wu, J., Jenkins, N., Janake, E.: 'Operating strategies for a GB integrated gas and electricity network considering the uncertainty in wind power forecasts', *IEEE Trans. Sust. Energy*, 2015, 5, pp. 128–138

[26] Midwest Independent System Operator, Midcontinent Independent System Operator. 'Business practices manual: energy and operating reserve markets'. January, 2016. https://www.misoenergy.org/_layouts/MISO/ECM/Redirect.aspx?ID=19178

[27] Correa-Posada, C.M., Sánchez-Martín, P.: 'Integrated power and natural gas model for energy adequacy in short-term operation', *IEEE Trans. Power Syst.*, 2015, 30 **No. 6**, pp. 3347–3355

[28] Markowitz, H.M., Manne, A.S.: 'On the solution of discrete programming problems', *Econometrica*, 1957, pp. 84–110

[29] Feng, Y., Rios, I., Ryan, S.M., Spurkel, K., Watson, J.P., Wets, R.J.B., et al.: 'Toward scalable stochastic unit commitment - part 1: load scenario generation', *Energy Syst.*, 2015, 6 **No. 3**, pp. 309–329

[30] Rios, I., Wets, R.J.B., Woodruff, D.L.: 'Multi-period forecasting and scenario generation with limited data', *Computat. Manage. Sci.*, 2015, 12 **No. 2**, pp. 267–295

[31] Sari, D., Lee, Y., Ryan, S., Woodruff, D.: 'Statistical metrics for assessing the quality of wind power scenarios for stochastic unit commitment', *Wind Energy*, 2009, 19 **No. 5**, pp. 873–893

[32] Bonneville Power Administration. 'Wind power forecasting data', 2015. Available from: http://www.bpa.gov/Projects/Initiatives/Wind/Pages/Wind-Power-Forecasting-Data.aspx

[33] Administration, Bonneville Power. 'Wind operational data', 2015. Available from: http://transmission.bpa.gov/Business/Operations/Wind/default.aspx

[34] Administration, Bonneville Power. 'Wind installed capacity', 2015. Available from: http://transmission.bpa.gov/Business/Operations/Wind/WIND.InstalledCapacity_DATA.pdf

[35] Papavasiliou, A., Oren, S.S., O'Neill, R.P.: 'Reserve requirements for wind power integration: A scenario-based stochastic programming framework', *IEEE Trans. Power Syst.*, 2011, 26 **No. 4**, pp. 2197–2206

[36] Wu, L., He, C., Dai, C., Liu, T.: 'Robust network hardening strategy for enhancing resilience of integrated electricity and natural gas distribution systems against natural disasters', *IEEE Trans. Power Syst.*, 2018, 33 **No. 5**, pp. 5787–5798

[37] The Renewable Energy Lab. 'Unit commitment data for modernized ieee rts-96'. The University of Washington. Available from: http://www.ee.washington.edu/research/real/library.html

[38] Morales-Espana, G., Latorre, J.M., Ramos, A.: 'Tight and compact MILP formulation for the thermal unit commitment problem', *IEEE Trans. Power Syst.*, 2013, 28 **No. 4**, pp. 4897–4908

[39] Hu, D., Ryan, S.M.: 'Datasets for stochastic vs. deterministic scheduling of a combined natural gas and power system with uncertain wind energy', *Mendeley Data, v1.* Available from: http://dx.doi.org/10.17632/6hdvk64kxs.1